Structural, optical and electrical properties of sulphide based heterojunction thin film

E. P. Obot[a], C. Augustine[a*], R. A. Chikwenze[a], S. O. Amadi[a], P. E. Okpani[b], P. N. Kalu[a], B. J. Robert[c], O.N. Nwoke[d], A.E. Igweoke[e], R. O. Okoro[f],
[a]*Department of Physics, Alex Ekwueme Federal University Ndufu-Alike, Ebonyi State, Nigeria*
[b]*Department of Electrical/Electronic Engineering, Alex Ekwueme Federal University Ndufu-Alike, Ikwo, Ebonyi State, Nigeria*
[c]*Department of Electrical/Electronic Engineering Technology, Akanu Ibiam Federal Polytechnic, Unwana, Ebonyi State, Nigeria*
[d]*Department of Mechanical Engineering, Akanu Ibiam Federal Polytechnic, Unwana, Ebonyi State, Nigeria*
[e]*Department of Mechanical Engineering, Alex Ekwueme Federal University Ndufu-Alike, Ikwo, Ebonyi State, Nigeria*
[f]*Department of Physics, Ikwo College of Education , Ebonyi State, Nigeria*

This contribution presents structural, optical and electrical properties of PbS/CdS thin films at different annealing temperatures. The XRD analysis reveal the existence of three different crystalline phases, i.e., the beta-CdS, hawleyite-CdS and greenockite-alpha-CdS phases within the CdS-shell of PbS/CdS core shell thin film. The dislocation density and microstrain decreased with annealing temperatures indicating a decrease in lattice imperfections and formation of high quality film and it can be attributed to the increase in grain size of the film with increase in annealing temperatures. Optical studies placed the band gaps at 1.25eV-1.75eV. About the same magnitude were found from electrical conductivity test. The samples exhibited high conductivity with increasing annealing temperatures which resulted to the bumping of electrons from the valence band to the conduction band. The high absorbance suggest that the film could be coated on collectors to enhance solar energy collection. The achieved band gaps placed the PbS/CdS fabricated with the presented method as a good material for solar photovoltaic applications.

(Received February 3, 2022; Accepted March 20, 2023)

Keywords: Absorbance, Temperature, Conductivity, Band gap, Thin film

1. Introduction

The need to harness the abundant solar energy resources cannot be overemphasized. The major problem is that despite the enormous quantum of energy available to mankind from the sun, it has remained inadequately harnessed and its present harvesting costs very high. For this reason, scientists in solid state and material science are researching with a view to finding suitable semiconductor materials that can give better conversion efficiency of the solar radiation into electricity at relatively low cost. The solar energy production is made possible by using a solar cell. A solar cell is a device that converts sun light energy to electricity via Photoelectric effect (Theraja, 2007). Silicon based solar cell tend to occupy the solar energy market, but thin film solar cell is currently gaining recognition due to its low cost in comparison to the high cost of silicon based solar cell which has made the entire production of solar energy to be expensive(Minami, 2005).

Semiconductors such as PbS and CdS are promising semiconductor materials for fabricating low-cost solar cells. These semiconductors have been obtained as polycrystalline thin films by several deposition techniques, one of the simplest being the chemical bath deposition [1].

* Corresponding author: emmyaustine2003@yahoo.com
https://doi.org/10.15251/JOR.2023.192.207

The chemical bath deposition (CBD) has been traditionally used to prepare thin films of chalcogenide semiconductors [2–8], CdS and PbS in particular. Most of these semiconductor compounds have interesting properties for device applications, including photovoltaics. For example, chemically deposited CdS is an important II – VI semiconductor having a wide band-gap of 2.4 eV with well-known applications in lasers, light-emitting diodes, solar cells, etc. [9]. CdS is used as a buffer material for high efficiency polycrystalline thin film solar cells [10]. Lead sulphide (PbS) is an important direct narrow gap semiconductor material with an approximate energy band gap of 0.4 eV at 300K and a relatively large excitation Bohr radius of 18 nm [11]. PbS has been widely studied because of its applications in infrared detection [12], utilized as solar control coatings [13, 14], and thin film solar cells [15-17].

There is considerable interest in the deposition of core-shell thin film material, due to the potential of tailoring both the lattice parameters and the band gap by controlling depositions parameters [18, 19]. 'The shell can alter the charge, functionality, and reactivity of surface, or improve the stability and dispersive ability. Furthermore, catalytic, optical, or magnetic functions can be imparted to the core particles by the shell material'. In general, the synthesis of core/shell structured material has the goal of obtaining a new composite material having synergetic or complementary behaviours between the core and shell materials [20].

Thin films of lead sulphide and cadmium sulphide are a promising photo voltaic materials as their variable band gap could be adjusted to match the ideal band gap (~1.5 eV) required for achieving a most efficient solar cell [21]. Extensive studies of the electrical and optical properties of PbS-CdS have been conducted by many researchers [22-27].

In this communication, we report the structural, optical and electrical properties of chemical bath deposited PbS/CdS heterostructure.

2. Experimental

PbS/CdS thin film was grown on ordinary glass slide substrates by CBD technique. First, PbS was deposited in a chemical bath which contained 5ml of 0.3M $Pb(NO_3)_2$, 5ml of 0.5M $SC(NH_2)_2$, 5ml of 0.5M NaoH and 30ml of distilled water put in that order into 50ml beaker. To have good quality thin films, cleaning of the substrate surface is very important. So the substrates were previously degreased in hydrochloric acid and then cleaned with distilled water. The cleaned substrates were vertically dipped into a 50ml beaker, containing the mixed solutions, for 30 minutes at constant temperature of 273K. To obtain the PbS/CdS core-shell, the PbS deposit already formed (core) was inserted in a mixture containing aqueous solutions of 20ml of 0.5M $CdSO_4$, 10ml of 0.5M $SC(NH_2)_2$, 2ml of pure ammonia and 30ml of distilled water into 100ml beaker. The deposition was allowed to proceed at 70^{o}C temperature for 60 minutes. Two of the deposited films were annealed in an oven at 473K and 673K respectively for 1hr. One of the samples was left un-annealed to serve as the control. The kinematics of the reaction of the complex ion formation and subsequent film deposition process are shown below:

$$Pb(NO_3)_2 + 4NaOH \longrightarrow [Pb(OH)_4]^{2+} + 4Na^+ + 2NO^{3-}$$

$$[Pb(OH)_4]^{2-} + SC(NH_2)_2 \longrightarrow PbS + 2OH^- + CN_2H_2 + 2H_2O$$

$$Cd[(NH_3)_4]^{2+} \rightleftharpoons Cd^{2+} + 4NH_3$$

$$(NH_2)_2CS + 2OH^- \longrightarrow CH_2N_2 + 2H_2O + S^{2-}$$

$$Cd^{2+} + S^{2-} \longrightarrow CdS$$

Energy dispersive X-ray flouresence (EDXRF) analysis was done to determine the elemental composition of the film. Structural studies were done with Rigaku Ultima IV X-ray diffractometer equipped with a graphite-monochromated CuK_α radiation source (40KV, 30mA), Four point probe Keithley model was used for the electrical characterization while thermo scientific GENESYS 10S model UV-VIS spectrophotometer on the 300-1000 nm range of light at

normal incidence to samples was used to obtain the absorbance data from which transmittance, reflectance, absorption coefficient and band gap were calculated.

3. Results and discussion

The XRD pattern of PbS/CdS heterostructure for the as-deposited, thermally annealed at 473K and 673K, are given in Figures 1, 2 and 3 respectively. The measurements showed that the heterostructure is polycrystalline. Such X-ray spectra display prominent peaks located at the following angular positions: 2θ = [25.964, 26.507, 27.858, 30.075, 30.808, 43.059, 43.760, 43.917, 43.942, 50.978, 51.911, 51. 942]. They are related with the reflection peaks of (111), (111), (420), (200), (200), (220), (444), (220), (722), (311), (311), (080) respectively. The diffraction peaks of 2θ = [25.964^o, 30.075^o, 43.059^o, 50.978^o] can be perfectly indexed to Galena PbS according to reference patterns JCPDS 05-0592. The peaks of 2θ values of 27.858^o, 43.760^o, 43.942^o and 51.942^o were identified to be CdS (JCPDS 00-047-1179). The peaks of 26.507^o, 30.808^o, 43.917^{o}and 51.911^{o}are attributed to Beta-CdS (JCPDS 00-001-0647). Other phases observed in the XRD patterns includes hawleyite-CdS (JCPDS 00-042-1411) associated with 2θ values of 26.515^o, 30.710^o, 43.984^o and 52.095^o corresponding to (111), (200), (220) and (311) reflections. Greenockite-α-CdS (JCPDS 00-001-0780) with angular positions of 24.993^o, 28.401^o, 43.693^o and 47.835^o corresponding to (100), (101), (110) and (103) reflections was also observed.

Table 1. The effects of annealing temperature on XRD parameters of PbS/CdS thin film

Samples	d-spacing (A)	D (nm)	δ $(nm)^{-2}x10^{-3}$	ε x 10^{-4}
As-deposited	3.4289	68.96	0.46	9.22
473K	2.9689	73.49	0.39	8.67
673K	2.0990	80.48	0.29	0.12

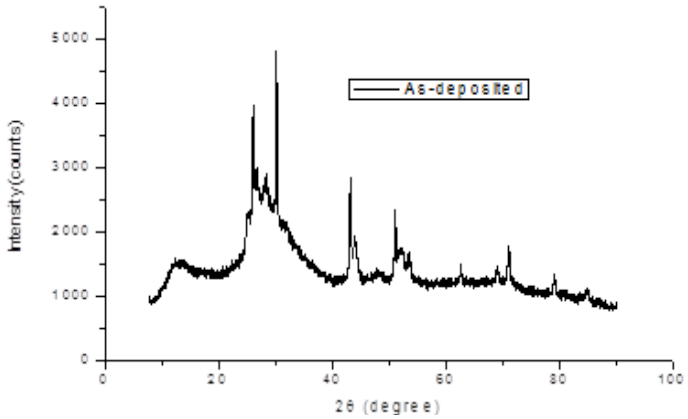

Fig. 1. XRD spectra of PbS/CdS as-deposited.

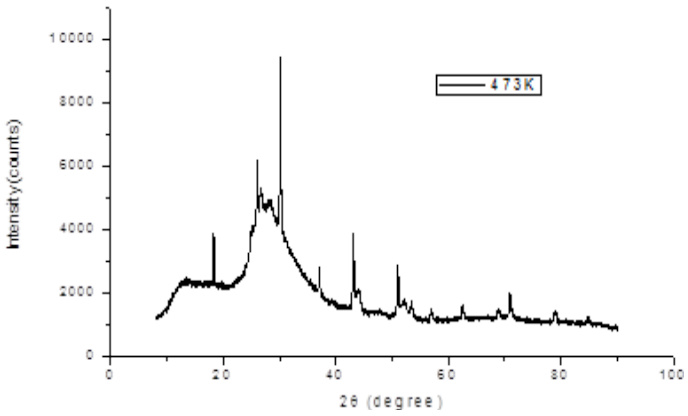

Fig. 2. XRD spectra of PbS/CdS annealed at 473K.

The strong peak intensity indicates the high degree of crystallinity of the films. The average grain size (D), microstrain (ε) and dislocation density (δ) were calculated for all the samples. The film annealed at 673K exhibited maximum crystallinity. 'Dislocation density values indicates the amount of defects in the structure'. 'Higher dislocation density values indicate lower crystallinity levels for the films'. The dislocation density was found to decrease with increase in annealing temperatures and was lowest for the 673K sample owing to the high crystalline nature of the film as obtained from the XRD analysis.

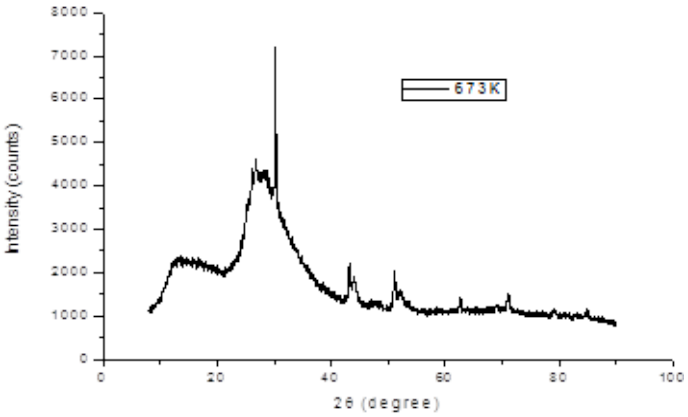

Fig. 3. XRD spectra of PbS/CdS annealed at 673K.

The grain size (D) and dislocation density (δ) were calculated using the relations [28, 29].

$$D = \frac{K\lambda}{\beta \cos\theta} \tag{1}$$

$$\delta = \frac{1}{D^2} \tag{2}$$

The decrease in microstructure (Table 1) with respect to increase in annealing temperatures indicate the decrease in lattice imperfection and formation of high quality film and it can be attributed to the increase in grain size of the film with increase in annealing temperatures. The microstrain was calculated using Williumson-Hall equation [30].

$$\beta \cos\theta = \frac{K\lambda}{D} + \varepsilon \sin\theta \tag{3}$$

where λ is x-ray wavelength in nm, β is the real diffraction broadening, K is a constant and is equal to 0.9, when β is measured at half-maximum of the diffraction peak and θ is the Bragg's angle. The XRD analysis showed that annealing temperatures play a vital role in the microstructure and the structural properties of PbS/CdS film samples.

Energy dispersive X-ray analysis (EDX) is one of the versatile techniques used for determining the chemical composition of unknown material, by identifying the peaks in EDX spectrum which is unique to an atom and therefore corresponds to a single element. The EDX analysis of PbS/CdS core /shell (Fig. 4) shows that lead (Pb) peak was recorded at 1.8keV, 2.4ke, 9.2keV, 10.6keV, 11.4keV, 12.6keV and 15.1keV, cadmium (Cd) peak at 4.0keV and sulphur (S) peak at around 2.4KeV.

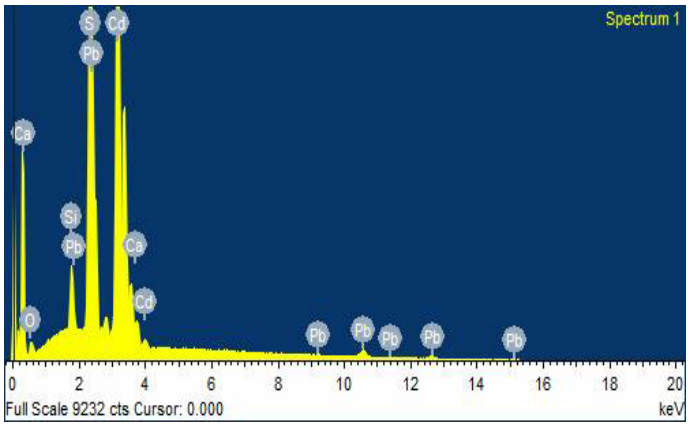

Fig. 4. EDXRF for PbS/CdS thin film.

The thickness of the film samples were calculated using the relation [31]

$$t = \frac{\left[\tan^{-1}\left[\frac{\left(n_o + n_g\right)^2 R - \left(n_o - n_g\right)^2}{\left(\frac{n_o n_g}{n} - n\right)^2 - \left(\frac{n_o n_g}{n} + n\right)^2 R}\right]^{\frac{1}{2}} \lambda\right]}{2\pi n} \tag{4}$$

where t is thickness, n_o is the refractive index of the medium of the incident light, which in this study is air, n_g is the refractive index of the substrate (glass in this case); and n is the refractive index of the thin film, R is reflectance and λ is wavelength.

The variation of absorbance (A) is studied in the wavelength range of 300-1000nm for all the deposited film. The other parameters which include transmittance (T), reflectance (R), absorption coefficient (α), band gap (E_g), extinction coefficient (k), are calculated using the relations available in literature [32]. Each parameter has its own significance and annealing has a marked effect on the optical properties. Transmittance and reflectance were calculated from the following relations [32]:

$$\mathrm{T} = \left(1 - R^2\right)\exp(-A) \tag{5}$$

$$R = 1 - \left[\mathrm{T}\exp(A)\right]^{\frac{1}{2}} \tag{6}$$

Absorption coefficient α was calculated from obtained data using the equation below:

$$\alpha = \frac{1}{t}\ln\frac{(1-R^2)}{\mathrm{T}} \tag{7}$$

And band gap was calculated using Tauc's relation:

$$(\alpha h\nu)^n = A\left(h\nu - E_g\right) \tag{8}$$

where A is band edge parameter and value of n determines the nature of optical transition (n = ½ indicates direct transition and n = 2 indicates indirect transition).

Optical absorption spectrum of polycrystalline PbS/CdS film deposited on transparent glass recorded in wavelength range 300-1000nm is shown in Fig.1. From the absorption spectrum, it is clear that the film samples have high absorbance of light across the studied electromagnetic spectrum. The as-deposited, thermally annealed at 473K and 673K all exhibited absorbance with peak of 4 (a.u). The peak for as-deposited occurs at 300-700nm range. The annealed at 473K exhibited peak corresponding to 300-780nm while that of the annealed at 673K corresponds to 300-850nm range. The absorbance spectra shows that the absorbance decreased sharply with increase in wavelength in the infrared region. The as-deposited decreased to about 2.75 (a.u). The annealed at 473K decreased to 1.85 (a.u) while the annealed at 673K decreased to 1.50 (a.u). The high absorbance of light especially in the visible region implies that the film could be applied as an absorbing material for solar thermal applications.

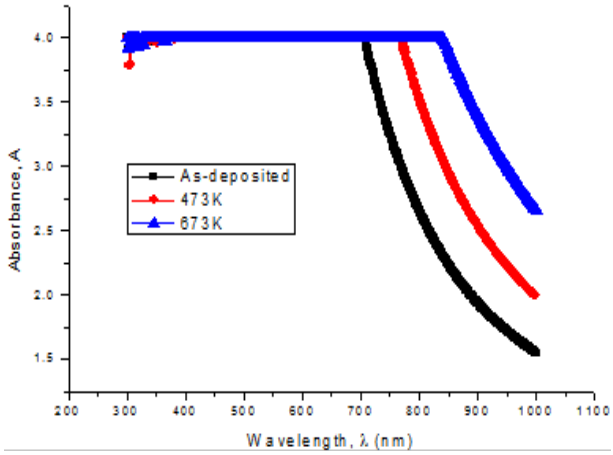

Fig. 1. Plots of absorbance against wavelength at different annealing temperatures.

The transmittance spectra changed with increasing annealing temperatures. It can be attributed to the change of thickness of the films due to the change of the grain size or an increase in the disorder of crystalline structures. Such transmittance spectra is shown in Fig. 2. It is concluded that the transmittance decreases with increasing annealing temperatures which is supported by the following reference in literature [33-35]. The plots of reflectance against wavelength at different annealing temperatures is shown Fig. 3. The film samples produce considerably low specular reflectance due to diffuse reflection from the surface.

The absorption coefficient of the film samples, calculated using equation (7), is presented in Fig. 4. The heated layers show higher values of absorption coefficient compared to the as-deposited. The increase in absorption coefficient with increase in annealing temperatures could

attributed to the distribution of the grains at various annealing temperatures. The concentration of carriers has also been reported to affect the absorption coefficient of thin films. Increase in temperature increases the carrier concentration and mobility of the charge carriers and this affects the absorption coefficient [36].

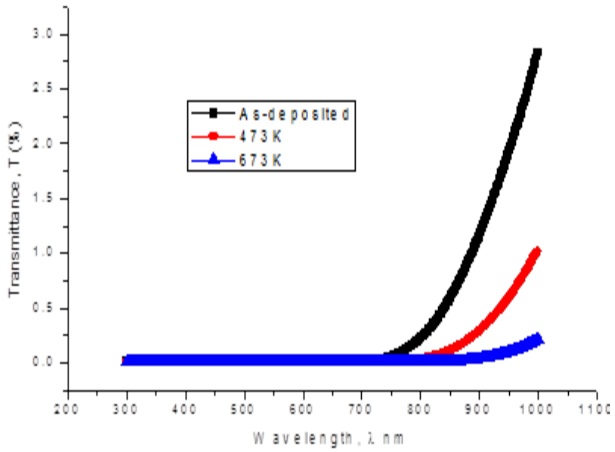

Fig. 2. Plots of transmittance of against wavelength at different annealing temperatures.

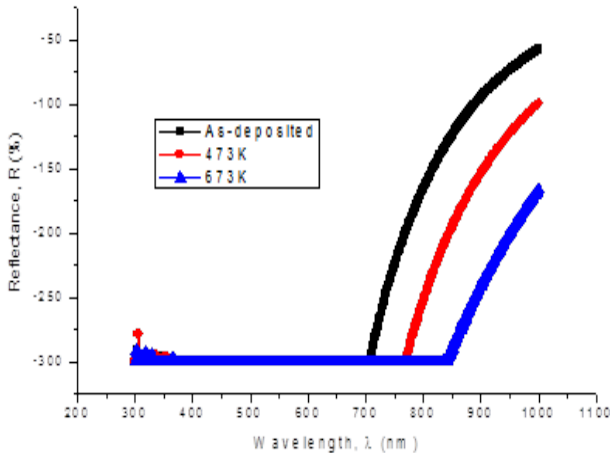

Fig. 3. Plots of reflectance against wavelength at different annealing temperatures.

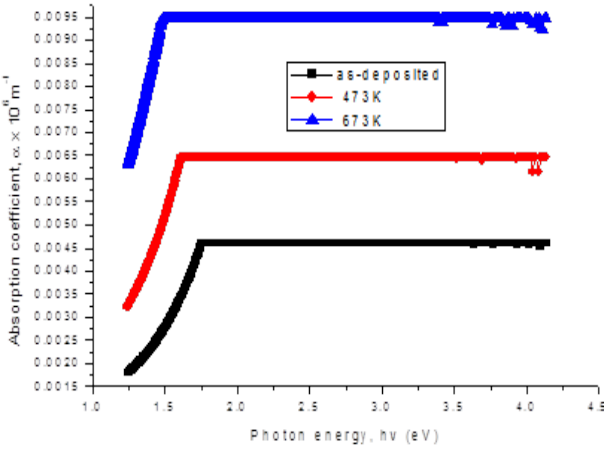

Fig. 4. Plots of absorption coefficient versus wavelength at different annealing temperatures.

The direct energy gaps value (E_g) for PbS/CdS film samples have been determined by using Tauc equation which is used to find the type of the optical transition. A plot of $(\alpha h\nu)^2$ against hυ for the deposited film samples is shown in Fig.5. The plot is linear indicating the direct band gap of the films. Extrapolation of straight line portion of the graph to the hν axis gives the band gap. The allowed direct band gap of as-deposited PbS/CdS thin film is 1.75eV while annealed PbS/CdS thin film, the allowed direct band gap is 1.65eV and 1.50eV at temperatures 473K and 673K respectively. As a result of annealing, the energy band gap decreased from 1.75eV to 1.50eV. Our finding in energy band gap were found slightly lower than those in the following reference which is 1.83eV [37]. However, they are in good agreement with Literature as given 1.65eV [38] and 1.61eV [39]. This change in band gap is explained in terms of quantum confinement effect [40]. These band gaps also exhibited similitude with lead sulphide coated with different shell materials (41, 42). Annealing clearly influenced the structural morphology of the films as denoted by the respective Urbach energies (the reciprocal of the gradient of natural log of absorption coefficient as a function of photon energy).

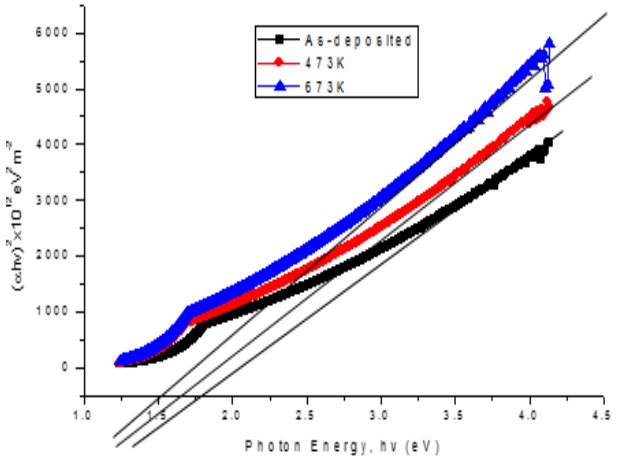

Fig. 5. Plots of $(\alpha h\nu)^2$ versus hν of PbS/CdS at different annealing temperatures.

Table 2. Summary of band gap of the film samples.

Property	*As-deposited*	*473K*	*673K*
Optical band gap (eV)	*1.75*	*1.50*	*1.25*
Electronic band gap (eV)	*1.79*	*1.57*	*1.28*
Urbach energy (eV)	*1.45*	*1.25*	*1.20*

Another important characteristics of the investigated PbS-CdS films which is electrical resistivity, seems to be significantly influenced by the annealing temperature. Lower electrical resistivity is usually characteristic for better crystalized films with large grains in which carrier transport is less influenced by grain boundaries [43, 44]. Table 3 shows the variation of resistivity with annealing temperatures for some representative samples of the deposited thin films. From the table 3, we found that the resistivity decreases with increasing annealing temperature. This could be attributed to the bumping of the electrons to the conduction band by thermal annealing and in doing so leaves a hole in the valance band. The decrease in the resistivity with temperature is mainly regarded as due to the thermally activated mobility of the carriers (e^- and e^+) [45]. On the other hand, ‘‘the conductivity of a semiconductor is determined by availability of free carrier concentrations and carrier mobility, while temperature is a measure of the average kinetic energy of the particles of a material, its follows that both carrier concentration, carrier mobility and electrical resistivity are sensitive to temperature’’. It is pertinent to note that the electrical properties of thin films is also related to the grain size. The growth in grains leads to the reduction of grain boundary scattering which decreases the resistivity for the films and eventually the increase in the conductivity of the films [46].

The electrical characterization of thin films are usually carried out with four point probe. The four point probe method is the most common way to measure a semiconductor material’s resistivity. Two of the probes are used to source current and the other two probes are used to measure voltage. The technique involves bringing four equally spaced probes into contact with the material of unknown resistance. The two outer probes source current, while the two inner probes sense the resulting voltage drop across the sample. The sheet resistance, R_s is given by [47].

$$R_s = 4.53 \times \frac{V}{I} \tag{9}$$

where V is the measured voltage between the two inner probes and I is the current passed through the outer probes. The resistivity, ρ was determined from the relation [48].

$$\rho = R_s \times t \tag{10}$$

where t is the thickness.

Table 3. Electrical parameters of PbS/CdS thin film at different annealing temperatures.

Sample	V/I x 10^5 (volt/amp)	Sheet resistivity x 10^5 (Ω)	Resistivity (Ωm)
As-deposited	7.06	31.98	6.39
473K	7.63	34.56	4.97
673K	1.17	5.30	0.11

The estimation of the band gaps from regression analyses was made possible using the conductivity data of the film samples which exhibited exponential characteristics of the form.

$$\sigma = A\exp\left(-\frac{E_g}{K_B T}\right) \tag{11}$$

The band gap thus deduced, are within the same order of magnitude as those of optical studies and listed in Table 2.

4. Conclusion

It can be opined that the determination of band gap of PbS/CdS thin films was successfully done, and the film samples exhibited high conductivity at elevated temperature. Not only has this demonstrated the possibility of controlling the band gap of PbS/CdS with thiourea but also influenced the optical behaviour of the material. Due to the band gap, the PbS/CdS as fabricated herein holds good promise in solar photovoltaic applications. The influence of annealing temperature on the structural and optical properties were also discussed.

References

[1] M.O. Ortuno-Lopez, J.J. Valenzuela-Jauregui, R. Ramirez-Bon, E. Prokhorov, J. Gonzale-Hernandez, Journal of Physics and Chemistry of Solid, 63, 665-668 (2002); https://doi.org/10.1016/S0022-3697(01)00210-4

[2] P. Nemec, I. Nemec, P. Nahalkova, Y. Nemcova, F. Trojanec, P. Maly, Thin Solid Films, 403-404, (2002); https://doi.org/10.1016/S0040-6090(01)01530-9

[3] T. Nakada, M. Mitzutani, Y. Hagiwara, A. Kunioka, Solar Energy Materials and Solar Cells, 67, 255-260 (2001); https://doi.org/10.1016/S0927-0248(00)00289-0

[4] C. D. Lokhande, E. H. Lee, K. D. Jung, Q. S. Joo, Materials Chemistry and Physics, 91, 200-204 (2005); https://doi.org/10.1016/j.matchemphys.2004.11.014

[5] M.B. Ortun˜o-Lopez, J.J. Valenzula-Jauregui, M. Sotelo-Lerma, A. Mendoza-Galvan, R. Ramı'rez-Bon, Thin Solid Films, 429, 34-39 (2003); https://doi.org/10.1016/S0040-6090(03)00144-5

[6] M.G. Sandoval-Paz, R. Ramı'rez-Bon, Thin Solid Films, 517, 6747-6752 (2009); https://doi.org/10.1016/j.tsf.2009.05.045

[7] M.B. Ortuno-Lopez, J.J. Valenzula-Jauregui, R. Ramirez-Bon, E. Prokhorov, J. Gonzalez-Hernandez, Journal of Physics and Chemistry Solids, 63, 665-668 (2002); https://doi.org/10.1016/S0022-3697(01)00210-4

[8] J.J. Valenzula-Jauregui, R. Ramirez-Bon, A. Mendoza-Galvan, M. Sotelo-Lerma, Thin Solid Films, 441, 104-110 (2003); https://doi.org/10.1016/S0040-6090(03)00908-8
[9] M. Dhanam, B. Kavitha, B. Maheswari, G. R. Jesna, Acta Phys. Pol. A, 119, 885 (2011); https://doi.org/10.12693/APhysPolA.119.885
[10] P. K. Nair, M.T.S Nair, V.M. Garcia, O.L. Arenas, Y. Pena, A. Castillo, I.T. Ayala,O. Gomezdaza, A. Nchez, J. Campos, H. Hu, R. Suarez, M.E .Rinc'on, Sol. Energ. Mat. Sol. C., 52 , 313 (1998).
[11] J.L. Machol , F.W. Wise, R.C. Patel, D.B. Tanner, Phys. Rev. B, 48, 2819 (1993); https://doi.org/10.1103/PhysRevB.48.2819
[12] P. Gadenne, Y. Yagil, G. Deutscher, J. Appl. Phys., 66 , 3019 (1989); https://doi.org/10.1063/1.344187
[13] P.K. Nair V.M. Garcia, A.B. Hernandez, M.T.S. Nair, J. Phys. D: Appl. Phys., 24, 1466-1472 (1991); https://doi.org/10.1088/0022-3727/24/8/036
[14] P. Ileana, N. Cristina, I. Violeta, E. Indrea, I. Bratu, Thin Solid Films 307, 240-244 (1997); https://doi.org/10.1016/S0040-6090(97)00304-0
[15] P. Nair, Sol. Energy Mater. Sol. Cells. 52, 313 (1998); https://doi.org/10.1016/S0927-0248(97)00237-7
[16] J.J. Valenzuela-Jauregui, R. Ramirez-Bon, G. Mendoza, M. Sotelo-Lerma, Thin Solid Films, 104, (2003); https://doi.org/10.1016/S0040-6090(03)00908-8
[17] J. Hernandez-Borja, Y. V. Vorobiev, R. Ramirez-Bon, Sol. Energy Mater.Sol. Cells, 95, 1882 (2011); https://doi.org/10.1016/j.solmat.2011.02.012
[18] B.R. Sankagal, C.D. Lokhande, Materials Chemistry and Physics; 14, 126 (2002).
[19] K. D. Rakesh, S. Mohan, S.K. Agarwal, H. K. Sehgal, Thin Solid Films, 80, 447-448 (2002).
[20] P.E. Agbo, M.N. Nnabuchi, Core-Shell TiO2/ZnO Thin Film: Preparation, Characterization and effect of temperature on some selected properties, Chalcogenide Letters, 8(4), 273-278 (2011).
[21] B.B. Nayak, H.N. Acharya, J. Mat. Sci. lett. 4, 651 (1985); https://doi.org/10.1007/BF00720058
[22] S.O. Ahmed, M. A. Mahdi, Z. Hassan, M. Bououdina, Superlattices and Microstructures, 52, 816-823 (2012); https://doi.org/10.1016/j.spmi.2012.06.024
[23] M.A. Manal, H.H. Noor, I.M. Hanaa, H.M. Ghuson, A.A. Kadhim, F.A. Ameer, Investigation of optical properties of the PbS/CdS thin films by thermal evaporation, Journal of Electron Devices, 12, 761-766 (2012).
[24] J. Hernández-Borja, Y.V. Vorobiev, R. Ramírez-Bon, Thin film solar cells of CdS/PbS chemically deposited by an ammonia-free process, Sol. Energy Materials & Solar Cells, 95, 1882-1888 (2011).
https://doi.org/10.1016/j.solmat.2011.02.012
[25] A.I. Oliva, R. Castro-Rodriguez, O. Solis-Canto, V. Sosa, P. Quintana, J.L. Pena, Comparative of properties of CdS thin films grown by two techniques, Applied surface science, 205, 54-56 (2003). https://doi.org/10.1016/S0169-4332(02)01081-4
[26] L. Lai-Hung, P. Loredana, V.K. Maksym, A.L. Maria, Sensitized solar cells with colloidal PbS-CdS core-shell Quantum Dots, Phys. Chem. Chem. Phys., 16, 736-742 (2014).
https://doi.org/10.1039/C3CP54145B
[27] W. K. Erich, Fabrication of All-Inorganic Optoelectronic Devices using Matrix Encapsulation of Nano Crystal Arrays, M.Sc Thesis, Graduate College of Bowling Green State University, 6-52 (2012).
[28] H.P. Klug, L.E. Alexander, X-ray diffraction procedure for polycrystalline and armophous materials, Wiley New York, (1974).
[29] K. O. Ovid, "Interfaces and misfit defects in nanostructured and polycrystalline films, Rev. Adv. Mater. Sci., 1, 61(2000).
[30] B. G. Jeyaprakash, K. Kesavan, K. Ashok, S. Mohan, A. Amalarami, Temperature dependent grain size and microstructure of CdO thin films prepared by spray pyrolysis method, Bull. Mater. Sci., 34, 601-605 (2011). https://doi.org/10.1007/s12034-011-0169-2

[31] M.N. Nnabuchi, Bandgap and optical properties of chemical bath deposited magnesium sulphide (MgS) thin films, Pacific Journal of Science and Technology, 6(2), 105-110 (2005).
[32] C. D. Lokhande, B.R. Sankapal, R.S. Mane, H.M. Pathan, M. Muller, M. Giersig, V. Ganesan, Appl. Surf. Sci., 193, 1 (2002). https://doi.org/10.1016/S0169-4332(01)00819-4
[33] P. E. Agbo, M. N. Nnabuchi, Core-Shell TiO2/ZnO Thin Film: Preparation, Characterization and effect of temperature on some selected properties, Chalcogenide Letters, 8 (4), 273 (2011).
[34] P. E. Agbo, G. F. Ibeh, S. O. Okeke, J. E. Ekpe, Chemically Deposited Cuprous Oxide Thin Film on Titanium Oxide for Solar Applications, Communications in Applied Sciences, 1 (1), 38 (2013).
[35] U. Cemal, E. Ozge, G. Mustafa, C. Gumus, Effect of annealing temperatures on the physical properties of Mn3O4 thin film prepared by chemical bath deposition, Int. J. Electrochem. Sci., 11, 2835-2845.
[36] A.L. Cai, J.F. Muth, Refractive index and other Properties of Doped ZnO Films, Mat. Res. Soc. Symp. Proc 764,120-140 (2003).
https://doi.org/10.1557/PROC-764-C3.21
[37] A.I. Onyia, M.N. Nnabuchi, Study of Optical properties of CdS/PbS and PbS/CdS Heterojunction Thin Films Deposited using Solution Growth Technique, Proceedings of the 1st African International Conferences/Workshop on Applications of Nanotechnology to Energy, Health and Environment, UNN, March 23-29, (2014).
[38] M.A. Manal, H.H. Noor, I.M. Hanaa, H.M. Ghuson, A.A. Kadhim, F.A. Ameer, Investigation of optical properties of the PbS/CdS thin films by thermal Evaporation, Journal of Electron Devices, 12, 761-766 (2012).
[39] H.Y. Deuk, M.L. Seung, H.J. Yem, M. Jooho, S.C. Yong, Origin of the enhanced photovoltaic characteristics of PbS thin film solar cells proceeded at near room temperature, Journal of Materials Chemistry A, 2, 20112-20117 (2014).
https://doi.org/10.1039/C4TA03433C
[40] T.O. Daniel, Effect of substrate temperature on zinc oxide doped aluminium, M.Sc Desertation, Federal University of Technology, Minna, Niger State (2015).
[41] C. Augustine, M. N. Nnabuchi, F. N. C. Anyaegbunam, A. N. Nwachukwu (2017). Study of the effects of thermal annealing on some selected properties of heterojunction PbS-NiO core-shell thin film, Digest Journal of Nanomaterials and Biostructures, 12 (2), 523-531.
[42] Augustine, C. and Nnabuchi, M.N. (2017). Band gap determination of novel PbS-NiO-CdO heterojunction thin film for possible solar energy applications, Journal of Ovonic Research, 13 (4), 233-240.
[43] M. Dhankhar, O.P. Singh, V.N. Singh, Physical principles of losses in thin film solar cells and efficiency enhancement methods, Renewable and Sustainable Energy Reviews 40, 214-223 (2014). https://doi.org/10.1016/j.rser.2014.07.163
[44] L. Wei, M.A. Ruixin, X. Jianshe, K. Bo, RF magnetron sputtered ZnO:Al thin films on glass substrates: a study of damp heat stability on their optical and electrical properties, Solar Energy Materials and Solar Cells, 91 (20), 1902-1905 (2007).https://doi.org/10.1016/j.solmat.2007.07.008
[45] P.E. Agbo, Growth and Characterization of Core-Shell Thin Films and Their Possible Applications, PhD. Thesis, Department of Industrial Physics, Ebonyi State University, (2012).
[46] O. Mustafa, Influence of grain size on the electrical and optical properties of lnP films, Chin. Phys. Lett, 25, (2008). https://doi.org/10.1088/0256-307X/25/11/069
[47] M.R. Islam, J. Podder, Optical properties of ZnO Nano Fibre Thin Films grown by Spray Pyrolysis of Zinc Acetate Precursor, Crystal Research Technology, 44 (3), 286-292 (2009).
https://doi.org/10.1002/crat.200800326
[48] B.L. Theraja, Textbook of Electrical Technology; S.C. Hard and Company Ltd, 243 - 2434 (2007).